

o-Nitrobenzyl Photolabile Protecting Groups with Red-Shifted Absorption: Syntheses and Uncaging Cross-Sections for One- and Two-Photon Excitation

Isabelle Aujard,^[a] Chouaha Benbrahim,^[a] Marine Gouget,^[a] Odile Ruel,^[a] Jean-Bernard Baudin,^[a] Pierre Neveu,^[a, b] and Ludovic Jullien*^[a]

Abstract: We evaluated the *o*-nitrobenzyl platform for designing photolabile protecting groups with red-shifted absorption that could be photolyzed upon one- and two-photon excitation. Several synthetic pathways to build different conjugated *o*-nitrobenzyl backbones, as well as to vary the benzylic position, are reported. Relative to the reference 4,5-dimethoxy-2-nitrobenzyl group, several *o*-nitrobenzyl derivatives exhibit a large and red-shifted one-photon absorption within the near-UV range. Uncaging after one-photon excitation was studied by measuring UV-visible absorption and steady-state fluorescence emission on model caged ethers and esters. In the whole series investi-

gated, the caged substrates were released cleanly upon photolysis. Quantum yields of uncaging after one-photon absorption lie within the 0.1–1% range. We observed that these drop as the maximum wavelength absorption of the *o*-nitrobenzyl protecting group is increased. A new method based on fluorescence correlation spectroscopy (FCS) after two-photon excitation was used to measure the action uncaging cross section for two-photon

excitation. The series of *o*-nitrobenzyl caged fluorescent coumarins investigated exhibit values within the 0.1–0.01 Goeppert–Mayer (GM) range. Such results are in line with the low quantum yields of uncaging associated with cross-sections of 1–50 GM for two-photon absorption. Although the cross-sections for one- and two-photon absorption of *o*-nitrobenzyl photolabile protecting groups can be readily improved, we emphasize the difficulty in enlarging the corresponding action uncaging cross-sections in view of the observed trend of their quantum yield of uncaging.

Keywords: acidity • basicity • cage compounds • donor–acceptor systems • fluorescence correlation spectroscopy

Introduction


Photolabile protecting groups have numerous applications in chemistry.^[1–3] The removal of this category of protecting groups is “clean”: in contrast to most other protecting strategies, release of the protected (“caged”) substrate requires no added reagent, only light. This feature is particularly fa-

vorable if access to the reaction site is difficult, or if chemical reagents are of restricted use. This is, for instance, the case with living organisms. In such systems, addressing biological issues often requires delivery of biologically active species at a given time and to a given location. This may be achieved by manipulating microsyringes. A noninvasive alternative involves adding to the biological medium caged compounds that reveal their biological activity only upon illumination. A pulse of a focussed laser beam provides temporal and spatial control over the delivery of the biologically active substrates.^[4]

To be useful in biological experiments, a caging group must fulfil various requirements. Some of these deal with nonphotophysical aspects, such as access of the caged substrates to the biological targets, or the absence of any “dark” biological activity. Others depend directly on photochemistry and photochemistry: photolysis of the caging group must be nondetrimental to the biological system, and it must occur faster than the process under investigation. The large number of engineering constraints has led to the con-

[a] Dr. I. Aujard, C. Benbrahim, M. Gouget, Dr. O. Ruel, Dr. J.-B. Baudin, P. Neveu, Prof. Dr. L. Jullien
Département de Chimie (C.N.R.S. U.M.R. 8640)
École Normale Supérieure
24, rue Lhomond, 75231 Paris Cedex 05 (France)
Fax: (+33) 144-323-325
E-mail: ludovic.jullien@ens.fr

[b] P. Neveu
Département de Physique (C.N.R.S. U.M.R. 8550)
École Normale Supérieure
24, rue Lhomond, 75231 Paris Cedex 05 (France)

 Supporting information for this article is available on the WWW under <http://www.chemurj.org/> or from the author.

tinuous introduction of new types of photolabile protecting groups.^[2,3,5–12]

Most caging groups absorb ultraviolet (UV) light. This is a major drawback if substrate release is induced by one-photon excitation. Indeed, the ubiquitous presence of UV light is damaging to cells as it is absorbed by intrinsic biological chromophores, especially DNA. A less-damaging release approach relies on two-photon infrared (IR) excitation. In addition to the better transparency of biological media to IR light, two-photon excitation confines substrate activation to the focal point of a laser beam, and the three-dimensional resolution achieved is higher than that with one-photon excitation. The efficiency of a protecting group that is photolabile upon two-photon excitation is evaluated by its action uncaging cross-section for two-photon excitation, $\delta_u\Phi_u^{(2)}$. This value is the product of the cross-section for two-photon absorption that leads to uncaging, δ_u , and the quantum yield of uncaging after two-photon excitation, $\Phi_u^{(2)}$. Although highly desirable for biological applications, improving the efficiency of a photolabile protecting group upon two-photon excitation remains difficult. Indeed, there

are no reliable rules for predicting the cross-section for two-photon absorption of a chromophore from its structure. In addition, it is difficult to predict the quantum yield of uncaging after two-photon excitation, even if the corresponding quantum yield of uncaging after one-photon excitation, $\Phi_u^{(1)}$, is known. Indeed, the mechanism leading to uncaging could depend on the excitation mode. According to biological applications, $\delta_u\Phi_u^{(2)}$ should exceed 0.1 Goeppert–Mayer (GM)^[7] or 10 GM,^[13] for which one GM unit is defined as $10^{-50} \text{ cm}^4 \text{ s photon}^{-1}$. The 1 GM range has already been obtained.^[7,8,14] In principle, 10–100 GM ranges in wavelength available from current-pulsed IR laser sources could be reached for reasonably “small” molecules by combining the largest ever observed values for the cross-section for two-photon absorption^[15,16] with the uncaging quantum yields.

Among the available photoremovable protecting groups, the 2-nitrobenzyl functionality has gained wide acceptance and most of the caged biologically active compounds that have been synthesized belong to this series.^[13,17–23] The mechanism leading to the photolytic release of the protected substrate has been extensively investigated both experimentally^[24–26] and theoretically.^[27] In contrast, 2-nitrobenzyl caged compounds have not attracted considerable attention regarding biological applications that rely specifically on two-photon excitation. In fact, the most widely used 2-nitrobenzyl protecting moieties require the blue edge of the wavelength range that is available with the laser sources commonly used for two-photon excitation. In addition, they exhibit rather small action uncaging cross-sections for two-photon absorption. For instance, $\delta_u\Phi_u^{(2)} \approx 0.01$ GM within the 700–750 nm range for the most popular 4,5-dimethoxy-2-nitrobenzyl group.^[7,28]

The present paper examines the 2-nitrobenzyl platform to conceive photolabile protecting groups with improved performances relying on both one- and two-photon excitation. The syntheses of two series of 2-nitrobenzyl alcohols is described. In the first series, we modified the backbone conjugated to the nitro group, with the aim of enlarging the maximum wavelength of absorption as well as the corresponding molar absorption coefficient.^[29] We evaluated independently the significance of a benzylic substituent in the second series.^[5,10,30] We then synthesized two series of caged model compounds that result from the protection of a phenol or a carboxylic acid group, respectively, and report the linear absorption and emission properties of these synthesized species. The action uncaging cross-sections for one- and two-photon excitation were measured. The latter were obtained by a new method based on fluorescence correlation spectroscopy (FCS) after two-photon excitation.

Design

Protecting groups: We designed two independent series of protecting groups based on the 2-nitrobenzyl platform. In principle, these were conceived to facilitate the design of improved protecting groups of second generation by combining the information collected from each series.

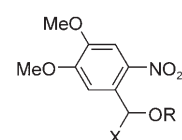
Abstract in French: Cet article évalue le squelette o-nitrobenzyle pour définir des groupements protecteurs photolabiles possédant une absorption déplacée vers le rouge qui peuvent être photolysés après excitation à un ou à deux photons. Nous décrivons plusieurs voies d'accès pour synthétiser différents squelettes o-nitrobenzyle conjugués, ainsi que pour modifier la position benzylique. Vis-à-vis du groupement protecteur de référence 4,5-diméthoxy-2-nitrobenzyle, plusieurs dérivés o-nitrobenzyle présentent une forte absorption déplacée vers le rouge se situant dans le proche UV. La photodéprotection après excitation à un photon a été étudiée par absorption UV-visible et par émission de fluorescence stationnaire sur des éthers et esters modèles cagés. L'intégralité des substrats cagés est efficacement déprotégée par photolyse. Les rendements quantiques de déprotection après excitation à un photon sont d'environ 0.1–1 %. Ils semblent diminuer lorsque la longueur d'onde d'absorption maximum du groupement protecteur o-nitrobenzyle augmente. Une nouvelle méthode reposant sur l'utilisation de la spectroscopie de corrélation de fluorescence après excitation biphotonique a été employée pour mesurer les sections efficaces de photodéprotection après excitation à deux photons. Celles de la série de coumarines fluorescentes cagées par nos groupements protecteurs o-nitrobenzyliques se situent dans la gamme 0.1–0.01 GM. Ces résultats sont en accord avec les faibles valeurs des rendements quantiques de photodéprotection associées à des sections efficaces d'absorption biphotoniques d'environ 1–50 GM. Alors qu'il est aisé d'augmenter les sections efficaces d'absorption à un et deux photons dans cette série, cette étude démontre qu'il est difficile d'améliorer les sections efficaces de photodéprotection correspondantes du fait de l'évolution des rendements quantiques de déprotection mise en évidence dans cet article.

In view of the wavelength range currently available with the common IR pulsed-laser sources, we were first concerned with red-shifting the UV absorption of the parent chromophore. Taking into account the presence of the electron-attracting nitro substituent on the aromatic ring, we grafted several conjugated electron-releasing moieties on the cycle.^[29] In addition, we introduced different conjugated paths between the donor and the acceptor groups. Beyond the anticipated red-shift, the corresponding donor–acceptor conjugated chromophores were expected to exhibit improved cross-sections for absorption at one- and two-photon.^[31,32] Scheme 1 displays the different backbones that were evaluated in the present study.

In parallel, we were also concerned with a possible drop in the quantum yield of uncaging that could be associated

dimethoxy-2-nitrobenzyl group. Scheme 2 shows the second series of molecules that were synthesized.

Caged model compounds: The design of the caged substrates was first governed by the nature of the groups to be protected. We chose to cage alcohol/phenols as well as carboxylic acids in view of the presence of both functions in many biologically active molecules. We additionally favored absorption



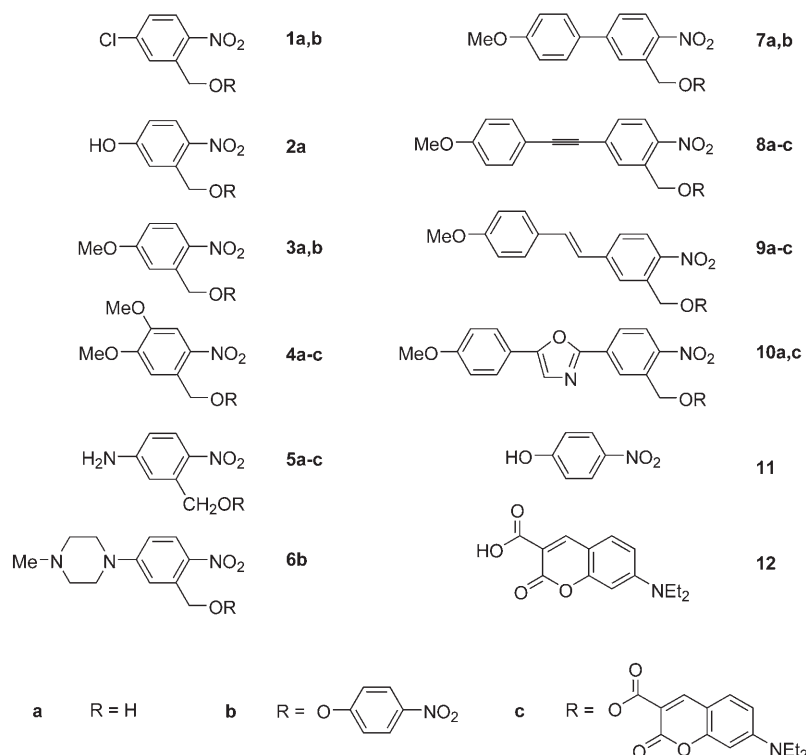
X=CF₃ **4Fa,c**

X=CCl₃ **4Cla,c**

X=CBr₃ **4Bra,c**

X=CN **4CNa,c**

Scheme 2. Generic structures of the second series of caging agents and caged model compounds.



Scheme 1. Generic structures of the first series of caging agents and caged model compounds.

with a red-shift of the absorption of the 2-nitrobenzyl protecting group. In fact, it was already known that the typical quantum yield of uncaging after one-photon absorption, $\Phi_u^{(1)}$, is reduced by more than one order of magnitude upon going from the 2-nitrobenzyl ($\Phi_u^{(1)} \approx 0.1$) to the 4,5-dimethoxy-2-nitrobenzyl group ($\Phi_u^{(1)} \approx 0.005$).^[7] Therefore, we also examined the effect of introducing a substituent at the benzylic position of the 2-nitrobenzyl protecting group. In fact, different reports suggested using this strategy to provide significant improvements over the parent compounds.^[5,10,30] In view of the nature of the substituents used in the latter studies, we chose to introduce electron-attracting substituents at the benzylic position of the popular 4,5-

and fluorescence emission of the caged substrates to access the action uncaging cross-sections for one- and two-photon excitation. This method requires consideration of the corresponding quantum yields of uncaging, as the photochemistry leading to substrate release may depend on the caged substrates (see below). At the same time, physicochemical experiments are facilitated, especially if two-photon excitation is used.

We first screened the series displayed in Scheme 1 by investigating the photolysis after one-photon absorption of caged derivatives of *p*-nitrophenol **11** (series **nb**). In its acidic state or as an alkyl ether, *p*-nitrophenol absorbs light of around 300 nm wavelength. In contrast, above its pK_a , *p*-nitrophenol exhibits a strong absorption that is red-shifted relative to the caged phenol ethers **nb**, as well as to

the subproducts that originate from the protecting group after photolysis. Thus, the action uncaging cross-section for one-photon excitation can be readily evaluated from the UV-visible absorption spectra.

We subsequently designed caged fluorescent compounds to measure the action uncaging cross-section for two-photon absorption for these protecting groups with sufficiently large molar-absorption coefficients above 350 nm. In fact, such donor–acceptor chromophores generally exhibit maxima of two-photon absorption, $\lambda_{\max}^{(2)}$, at wavelengths close to twice the corresponding maxima of one-photon absorption, $\lambda_{\max}^{(1)}$.^[31,32] In addition, the currently accessible excitation wavelength range for most femtosecond pulsed-laser sources

that are used for two-photon applications is 700–1000 nm. We chose to cage a fluorescent coumarin carboxylic acid **12** (series **nc**; Schemes 1 and 2). Its favorable photophysical features made it possible 1) to investigate its release by monitoring UV-visible absorption and fluorescence emission during the experiments relying on one-photon absorption; 2) to develop a new protocol for measuring the action uncaging cross-section for two-photon absorption that relies only on the observation and analysis of fluorescence emission from the focal point of the laser.

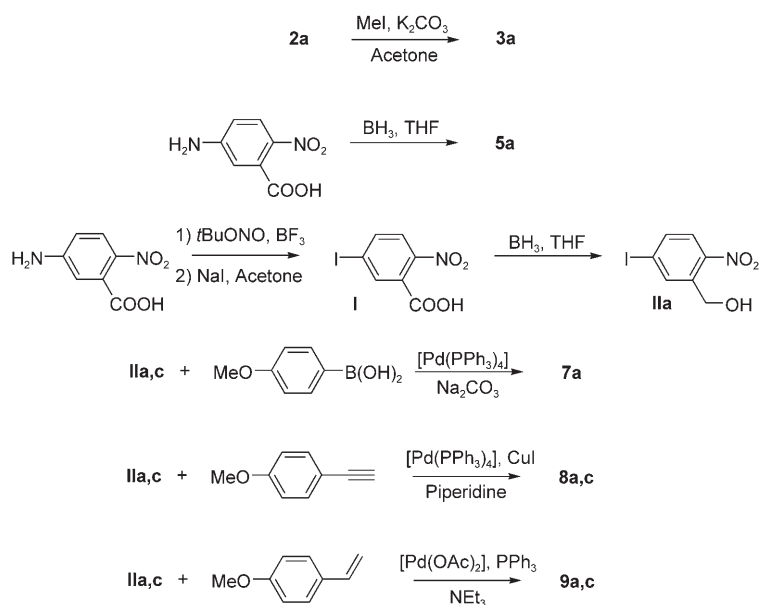
Syntheses

Photolabile protecting groups: 2-Nitrobenzyl alcohols were chosen as synthetic entries for the protecting groups based on the 2-nitrobenzyl platform (Scheme 3).

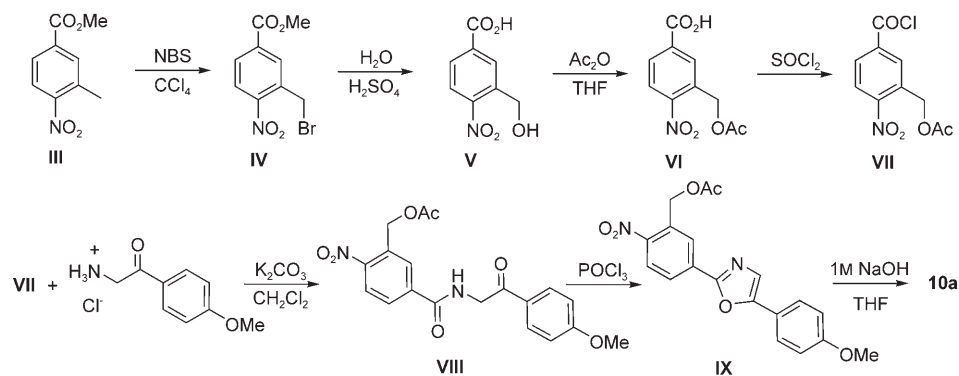
The 5-chloro-2-nitrobenzyl **1a**, 5-hydroxy-2-nitrobenzyl **2a**, and 4,5-dimethoxy-2-nitrobenzyl **4a** alcohols were commercially available. 5-Methoxy-2-nitrobenzyl alcohol **3a** was obtained by alkylation of the phenol **2a** with methyl iodide in the presence of dry potassium carbonate in acetone in 50% yield. The reduction of the commercially available 5-amino-2-nitrobenzoic acid with borane in THF gave 5-amino-2-nitrobenzyl alcohol **5a** in 83% yield.^[33] The 2-nitrobenzyl alcohols **7a**, **8a**, and **9a** were obtained from reaction of appropriate synthons with the 5-iodo-2-nitrobenzyl alcohol intermediate **IIa**. The latter was obtained in two steps from 5-amino-2-nitrobenzoic acid by 1) diazotation with *tert*-butyl nitrite followed by nucleophilic substitution with iodide to provide 5-iodo-2-nitrobenzoic acid **I** (yield: 65%);^[34] 2) reduction by borane in THF (yield: 90%).^[33] Compounds **7a**, **8a**, and **9a** were synthesized by coupling **IIa** with 4-methoxyphenylboronic acid, 4-ethynylanisole, and 4-methoxystyrene, respectively, in the presence of a palladium catalyst to give yields of 78, 89, and 34%, respectively.

The synthesis of {5-[5-(4-methoxyphenyl)oxazol-2-yl]-2-nitrophenyl}methanol (**10a**) relied on the condensation between 4-methoxy-2'-aminoacetophenone and acetic acid 5-

chlorocarbonyl-2-nitrobenzyl ester **VII** (Scheme 4). The latter was obtained in five steps from 3-methyl-4-nitrobenzoic acid: 1) esterification with methanol gave 3-methyl-4-nitrobenzoic acid methyl ester **III** (yield: 79%);^[35] 2) the ester **III** was brominated by *N*-bromosuccinimide (NBS) to afford 3-bromomethyl-4-nitrobenzoic acid methyl ester **IV** (yield: 12%);^[35] 3) **IV** was subsequently hydrolyzed to provide 3-hydroxymethyl-4-nitrobenzoic acid **V** (yield: 84%); 4) the benzylic alcohol **V** was esterified by acetic anhydride in THF to give the corresponding acetate, 3-acetoxymethyl-4-nitrobenzoic acid **VI** (yield: 92%); 5) **VI** was eventually treated by thionyl chloride to yield **VII** in quantitative yield. Acetic acid 5-[2-(4-methoxyphenyl)-2-oxo-ethyl carbamoyl]-2-nitrophenyl ester **VIII** was prepared from **VII** and 4-methoxy-2'-aminoacetophenone in 71% yield. Then **VIII** was dehydrated in phosphoryl chloride to give acetic acid 5-[5-(4-methoxyphenyl)-2-oxazol-2-yl]-2-nitrobenzyl ester **IX** (yield: 36%) that was eventually hydrolyzed to provide **10a** in 13% yield.

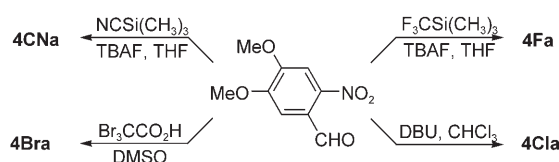


Scheme 3. Syntheses of the caging agents of the first series.



Scheme 4. Synthesis of **10a**.

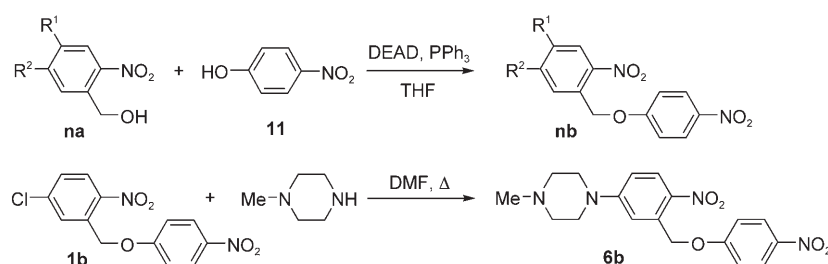
The syntheses of the 2-nitrobenzyl alcohols substituted in the benzylic position: **4Fa**, **4Cla**, **4Bra**, and **4CNa**, proceeded via the same 4,5-dimethoxy-2-nitrobenzaldehyde intermediate (Scheme 5). 2,2,2-Trifluoro-1-(4,5-dimethoxy-2-nitrophenyl)ethanol **4Fa** and hydroxy(4,5-dimethoxy-2-nitrophenyl)acetonitrile **4CNa** were prepared by reaction of 4,5-dimethoxy-2-nitrobenzaldehyde with (trifluoromethyl) trimethylsilane^[36] and trimethylsilane cyanide, respectively, in THF in 80 and 90 % yield. Condensation of chloroform on 4,5-dimethoxy-2-nitrobenzaldehyde in the presence of 1,8-diazabicyclo[5.4.0]undec-7-ene (DBU) gave 2,2,2-trichloro-1-(4,5-dimethoxy-2-nitrophenyl)ethanol **4Cla** in 98 % yield.^[37] Eventually, 2,2,2-tribromo-1-(4,5-dimethoxy-2-nitrophenyl)ethanol **4Bra** resulted from the decarboxylative condensation of tribromoacetic acid on 4,5-dimethoxy-2-nitrobenzaldehyde, in 88 % yield.^[38]



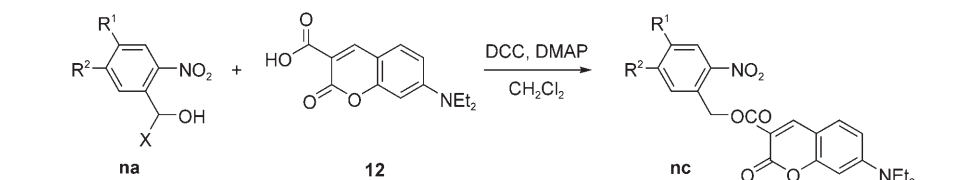
Scheme 5. Syntheses of the caging agents of the second series. TBAF = tetrabutylammonium fluoride, DMSO = dimethyl sulfoxide.

Caged model compounds: With the exception of **6b**, the 2-nitrobenzyl ethers of *p*-nitrophenol, **nb**, were obtained from the Mitsunobu reaction^[39,40] between *p*-nitrophenol **11** and the corresponding 2-nitrobenzyl alcohols, **na**, in moderate to good yields (Scheme 6). In contrast, 1-(4-nitrophenoxymethyl)-5-(*N*-methylpiperazine)-2-nitrobenzene **6b** was prepared directly from the nucleophilic substitution of 1-methylpiperazine on 1-(4-nitrophenoxymethyl)-5-chloro-2-nitrobenzene **1b** (78 % yield).^[29]

The 2-nitrobenzyl esters of the coumarine **12**^[41] were obtained by condensation between **12** and the corresponding 2-nitrobenzyl alcohols **na** (**n** = **II**, **4**, **4F**, **4Cl**, **4Br**, **4CN**, **5**, **10**) in the presence of *N,N'*-dicyclohexylcarbodiimide (DCC) (Scheme 7).



Scheme 6. Syntheses of the caged derivatives of the model phenol **11**. DEAD = diethyl azodicarboxylate.



Scheme 7. Syntheses of the caged derivatives of the model carboxylic acid **12**. DMAP = 4-dimethylaminopyridine.

Results

Linear absorption and emission properties

One-photon absorption: Here, we focus on the absorption properties of the 2-nitrobenzyl alcohols **na**. In fact, many substrates of biological interest do not absorb light of wavelengths within the range of absorption of the present 2-nitrobenzyl protecting groups.

The series of 2-nitrobenzyl alcohols **na** displayed in Scheme 1 exhibits one-photon absorptions within the UV range (Figure 1 and Table 1). The longest maximum wavelengths of absorption were observed for **9a** and **10a** ($\lambda_{\text{max}}^{(1)} \approx 370$ nm). In fact, the absorption band of both compounds extends up to 450 nm, as shown in Figure 1. Their molar absorption coefficients at the wavelength of maximum absorption are significantly larger than that of the reference derivative **4a**: $\epsilon(\lambda_{\text{max}}^{(2)}) \approx 2 \times 10^4 \text{ M}^{-1} \text{ cm}^{-1}$ versus $6 \times 10^3 \text{ M}^{-1} \text{ cm}^{-1}$. In addition, it remains larger than $10^4 \text{ M}^{-1} \text{ cm}^{-1}$ at 400 nm (Table 1). The maximum wavelength of absorption, as well as the molar absorption coefficient, of the 5-amino-2-nitrobenzyl alcohol **5a** are also noticeably larger than those of **4a**. As shown in Figure 1 and in Table 1, the triple-bond-containing alcohol **8a** absorbs within the same range of wavelengths as **4a**, albeit more intensively. As anticipated from the lower donating power of the donor conjugated to the nitro group, the other alcohols essentially absorb light at significantly shorter wavelengths than **4a**.

Except for some possible hypochromic or hyperchromic effects, the absorption spectra of the caged compounds compare satisfactorily with the sum of the respective absorption spectra of the *o*-nitrobenzyl moiety **na** and of the caged substrate. The absorption properties of these caged substrates can be compared to those of **3a** (**nb** series), or to the acidic state of **12** (**nc** series). In particular, we did not observe any alteration of band shape that could evidence a regime of strong coupling between the two chromophores that are present in both **nb** and **nc** series.^[42] Chromophore coupling was already invoked to account for a rather singular uncaging behavior in a 2-nitrobenzyl ester of a coumarine.^[43]

Steady-state fluorescence emission: The fluorescence emission

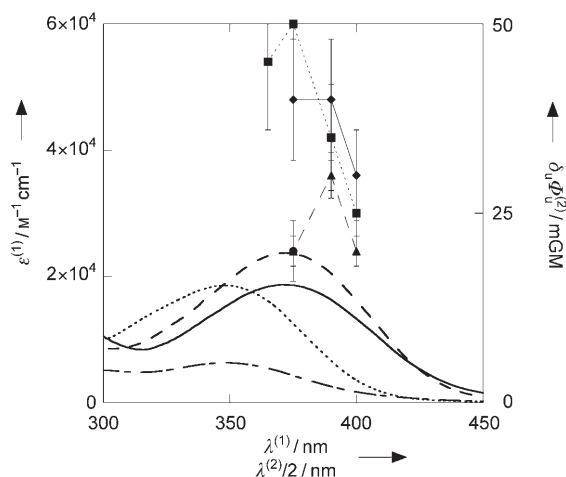


Figure 1. Photophysical properties of **4** (--- and ●), **8** (..... and ■), **9** (--- and ▲), and **10** (— and ♦) at 293 K. Single-photon absorption (**na** series; molar absorption coefficient ϵ in $\text{M}^{-1}\text{cm}^{-1}$; lines) and action uncaging cross-section for two-photon excitation (**nc** series; $\delta_u \Phi_u^{(2)}$ in mGM; symbols). Solvent: acetonitrile (one-photon excitation) and acetonitrile/Tris pH 9 buffer (20 mM) 1:1 (v/v) (two-photon excitation).

Table 1. Absorption and emission properties of the caging agents **na** and of the caged model compounds **nb** and **nc**. Maxima of single-photon absorption $\lambda_{\text{max}}^{(1)}$ and of steady-state fluorescence emission after one-photon excitation $\lambda_{\text{em}}^{(1)}$, molar absorption coefficients for single-photon absorption at $\lambda^{(1)}$, $\epsilon(\lambda^{(1)})$ ($\pm 5\%$), quantum yields of fluorescence after one-photon excitation $\Phi_F^{(1)}$ ($\pm 10\%$). Solvent: acetonitrile for measurements for **na**; acetonitrile/Tris pH 9 buffer (20 mM) 1:1 (v/v) in all other cases.

n	$\lambda_{\text{max}}^{(1)}(\text{na})$ [nm]	$\epsilon(\lambda_{\text{max}}^{(1)}), \epsilon(350),$ $\epsilon(400)$ (na) [$\text{mm}^{-1}\text{cm}^{-1}$]	$\lambda_{\text{max}}^{(1)} [\epsilon(\lambda_{\text{max}}^{(1)})](\text{nb})$ [nm] [$\text{mm}^{-1}\text{cm}^{-1}$]	$\lambda_{\text{max}}^{(1)} [\epsilon(\lambda_{\text{max}}^{(1)})](\text{nc})$ [nm] [$\text{mm}^{-1}\text{cm}^{-1}$]	$\lambda_{\text{em}}^{(1)} [\Phi_F^{(1)}](\text{nc})$ [nm] [%]
1	272	6, 0.4, 0.03	300 [14]	—	—
2	310	9, 3, 2	—	—	—
3	310	8, 2, 0.07	309 [21.9]	—	—
4	348	6, 6, 2	311 [17.9]	421 [18]	472 [0.4]
4F	342	5, 5, 1	—	433 [28]	473 [0.1]
4Cl	345	6, 6, 1	—	433 [29]	473 [0.1]
4Br	343	6, 6, 1	—	433 [27]	473 [0.2]
4CN	346	5, 5, 1	—	434 [20]	475 [0.2]
5	367	16, 14, 6	374 [14.5]	426 [23]	472 [0.4]
6	—	—	394 [16.3]	—	—
7	336	14, 12, 1	317 [29.0]	—	—
8	348	19, 19, 4	320 [19.2]	427 [49]	472 [0.2]
9	370	24, 20, 16	375 [23.4]	424 [47]	469 [0.05]
10	371	19, 16, 13	—	425 [46]	467 [0.02]
11	—	—	403 [16] ^[a]	—	—
12	—	—	—	405 [27] ^[a,b]	463 [8.5] ^[a,b]

[a] Values obtained in acetonitrile/Tris pH 9 buffer (20 mM) 1:1(v/v) for **11** and **12**. [b] In acetonitrile/Tris pH 2 buffer (20 mM) 1:1 (v/v) in which the acidic state is present, we observed $\lambda_{\text{max}}^{(1)} [\epsilon(\lambda_{\text{max}}^{(1)})]=422$ [35] and $\lambda_{\text{em}}^{(1)} [\Phi_F^{(1)}]=474$ [2].

of caged compounds may be significant for diverse applications. For instance, in biology, it may be essential to avoid any interference between the fluorescence emission from the starting caged molecule and that from the released substrate (tracer applications) or from any species produced after substrate release (detection of a biological response to a stimulus).

As shown in Table 1, the fluorescence emission of the 2-nitrobenzyl esters **nc** occurs at wavelengths similar to those for the case of the acidic state of **12**, which is a good photo-

physical model for esters of **12**. In contrast, the quantum yields of fluorescence emission from the **nc** caged coumarins are about one order of magnitude lower than the quantum yield of fluorescence of the acidic form of **12**. This observation probably reflects the quenching of the coumarin emission by the nitro group.^[43] Beyond its relevance to the applications mentioned above, this latter feature is favorable in the application of the method of measurement of the action uncaging cross-section for two-photon excitation that we introduce below.

Irradiation experiments with one-photon excitation: The model that was used to analyze the kinetics of uncaging of the **nb** and **nc** caged derivatives is detailed in the Experimental Section. In principle, the analysis is much simplified if excitation is performed at an isosbestic point in the absorption spectrum during the photoconversion of a caged compound into the released substrate. Nevertheless, the excitation wavelength $\lambda_{\text{exc}}^{(1)}$ plays no significant role as long as the total absorbance at the corresponding wavelength remains significantly lower than a value of one.^[44] We paid attention to fulfil the preceding condition for the present experiments.

All irradiations with one-photon excitation that are reported were performed at $\lambda_{\text{exc}}^{(1)}=325$ nm in acetonitrile/20 mM Tris pH 9 buffer 1:1 (v/v).

Figures 2a and 3a display typical evolutions of the absorbance of solutions of **8b** and **8c**, respectively, as a function of time upon illumination at 325 nm. In Figure 2a, one observes the continuous drop in the absorption of **8b** and an increase in absorbance within the 400 nm range that is in line with the absorption properties of the released 4-nitrophenate anion originating from **11** (see Table 1). In Figure 3a, the absorbance of **8c** decreases as a function of time and the absorbance that progressively increases at around 400 nm is in

agreement with the formation of the released basic state of the coumarin **12**. In the case of **8c**, it is also possible to follow the evolution of the system by monitoring fluorescence emission. Irradiation is associated here with an increase and a blue-shift of fluorescence emission, both of which are expected upon releasing the basic state of the coumarin **12**.

As shown in Figure 2b, the temporal evolutions of the absorbances within the respective wavelength ranges of absorption for **8b** and for the 4-nitrophenate anion were fitted

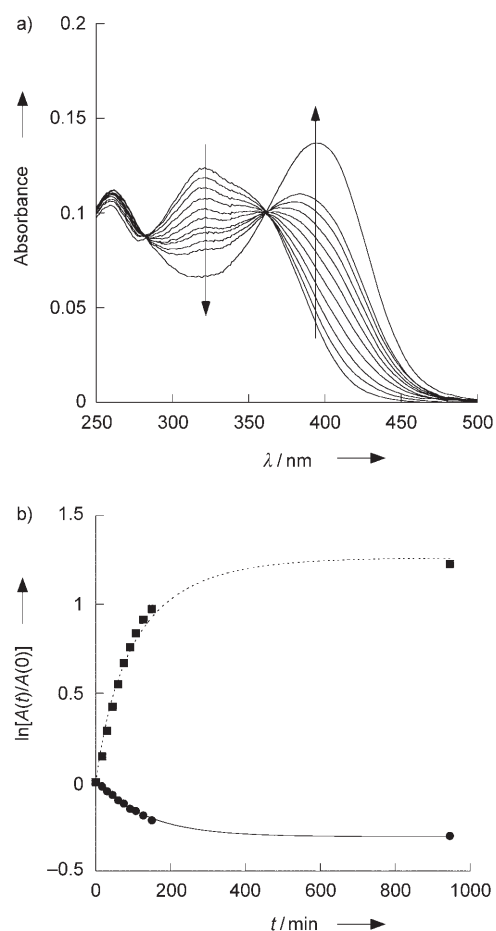


Figure 2. One-photon irradiation ($\lambda_{\text{exc}}^{(1)}=325$ nm) of a 4.9 μM solution of **8b** in acetonitrile/20 mM Tris pH 9 buffer 1:1 (v/v) at 293 K. a) Evolution of the UV-visible absorption spectra of the solution as a function of time ($t(\text{min})=0, 17, 30, 45, 60, 75, 92, 107, 127, 150, 946$); b) logarithmic plot of the total absorbance at 348 nm (\bullet , —) and at 395 nm (\blacksquare ,), as a function of time. Symbols: experimental points; lines: fits according to Equation (8), to give $k=7.9\pm0.8\times10^{-3}\text{ min}^{-1}$ (348 nm) and $k=6.2\pm0.6\times10^{-3}\text{ min}^{-1}$ (395 nm).

satisfactorily with Equation (8) derived from the kinetic model (see Experimental Section). We calculated the following respective rate constants for photolysis: $7.9\pm0.8\times10^{-3}\text{ min}^{-1}$ (analysis at 348 nm) and $6.2\pm0.6\times10^{-3}\text{ min}^{-1}$ (analysis at 395 nm). These values were in reasonable agreement and the average was accordingly used for further treatments. Similar behaviors were observed for the whole series of irradiation experiments performed on the **nb** caged ethers. Table 2 summarizes the values of the action uncaging cross-section for one-photon excitation at $\lambda_{\text{exc}}^{(1)}=325$ nm in the **nb** series, $\epsilon_u(325)\Phi_u^{(1)}(\text{nb})$. Photolysis rates that were too low rendered it impossible to measure reliably the corresponding action uncaging cross-section for one-photon excitation for the amino caged ethers **5b** and **6b**, as well as for the double-bond-containing derivative **9b**.

As illustrated in Figure 3c, the evolution of the absorbance and the fluorescence emission as a function of time were also accounted for satisfactorily by Equations (8,9) in

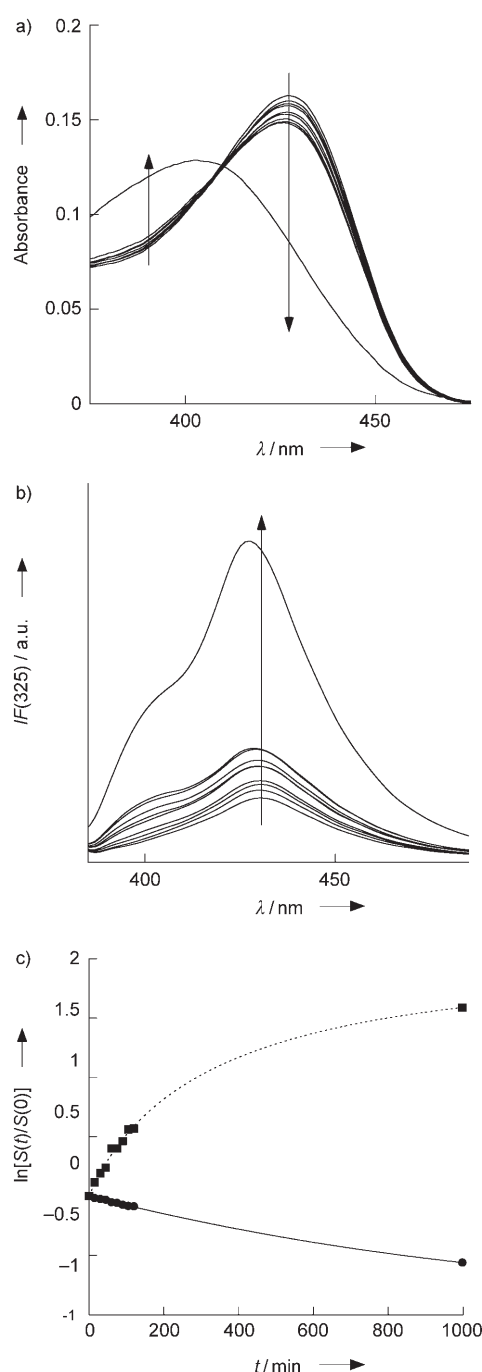


Figure 3. One-photon irradiation ($\lambda_{\text{exc}}^{(1)}=325$ nm) of a 3.3 μM solution of **8c** in acetonitrile/20 mM Tris pH 9 buffer 1:1 (v/v) at 293 K. a) Evolution of the UV-visible absorption spectra of the solution as a function of time ($t(\text{min})=0, 15, 30, 45, 60, 75, 90, 105, 120, 998$); b) evolution of the fluorescence emission spectra of the solution as a function of time ($t(\text{min})=0, 15, 30, 45, 60, 75, 90, 105, 120, 998$) ($\lambda_{\text{exc}}^{(1)}=325$ nm); c) logarithmic plot of the total absorbance at 425 nm (\bullet , —) and of the fluorescence emission at 460 nm (\blacksquare ,), as a function of time. Symbols: experimental points; lines: fits according to Equations (8,9) to give $k=1.4\pm0.1\times10^{-3}\text{ min}^{-1}$ from both fits.

the series of caged coumarin **nc**. The rate constants that were obtained from the analysis of the absorbance and of the fluorescence emission were in good agreement. For in-

Table 2. Action uncaging cross-section for one-photon excitation at $\lambda_{\text{exc}}^{(1)} = 325 \text{ nm}$, $\epsilon_u(325)\Phi_u^{(1)} (\pm 5\%)$, and estimate of the quantum yields of uncaging after one-photon excitation $\Phi_u^{(1)} (\pm 10\%)$ for the caged model compounds **nb** and **nc**; estimate of the action uncaging cross-section for one-photon excitation of the present *o*-nitrobenzyl protecting groups at $\lambda_{\text{exc}}^{(1)}$, $\epsilon_u(\lambda_{\text{exc}}^{(1)})\Phi_u^{(1)}$; action uncaging cross-section for two-photon excitation at $\lambda_{\text{exc}}^{(2)} = 750 \text{ nm}$, $\delta_u(750)\Phi_u^{(2)} (\pm 20\%)$ ($1 \text{ GM} = 10^{-50} \text{ cm}^4 \text{ s} (\text{photon})^{-1}$), for the caged model compounds **nc**; relative brightness of **ncA**[−] with respect to **nc** after two-photon excitation at the two-photon excitation wavelength $\lambda_{\text{exc}}^{(2)} = 750 \text{ nm}$, $\alpha(750) = \delta(750, \text{ncA}^-)/\delta(750, \text{nc})\Phi_F^{(2)}(\text{ncA}^-)/\delta(750, \text{nc})\Phi_F^{(2)}(\text{nc}) (\pm 20\%)$. Solvent: acetonitrile/Tris pH 9 buffer (20 mM) 1:1 (v/v). See text and Experimental Section for details.

n	$\epsilon_u(325)\Phi_u^{(1)}(\text{nb})$ [M ^{−1} cm ^{−1}]	$\epsilon_u(325)\Phi_u^{(1)}(\text{nc})$ [M ^{−1} cm ^{−1}]	$\Phi_u^{(1)}(\text{nb})^{[a]}$ [%]	$\Phi_u^{(1)}(\text{nc})^{[a]}$ [%]	$\epsilon_u(350)\Phi_u^{(1)}$, $\epsilon_u(400)\Phi_u^{(1)[b]}$ [M ^{−1} cm ^{−1}]	$\delta_u(750)\Phi_u^{(2)}(\text{nc})$ [mGM]	$\alpha(750)$
1	76	—	10	—	40, 3	—	—
3	46	—	0.7	—	14, 0.5	—	—
4	39	14	0.8	0.6	48, 16	20	150
4F	—	12	—	0.4	—	15	1000
4Cl	—	29	—	1.1	—	20	800
4Br	—	42	—	1.3	—	65	— ^[c]
4CN	—	7	—	0.3	—	20	—
5	— ^[d]	— ^[d]	—	— ^[d]	—	35	450
6	— ^[d]	—	—	—	—	—	—
7	70	—	0.5	—	65, 4	—	—
8	76	16	0.5	0.1	59, 12	50 ^[e]	1200
9	— ^[d]	11	—	0.1	—	20 ^[f]	800
10	—	10	—	0.1	—	40 ^[g]	2500

[a] $\Phi_u^{(1)} = \frac{\epsilon_u(325)\Phi_u^{(1)}}{\epsilon(325)(\text{na})}$, see text. [b] $\epsilon_u = \epsilon(\text{na})$ and $\Phi_u^{(1)} = \Phi_u^{(1)}(\text{nb})$. [c] The precision of α is too low to be reliable for the caged compounds with the largest $\delta_u(750)\Phi_u^{(2)}$ values. [d] Under our experimental conditions, uncaging was too slow to derive reliable values. [e] $\delta_u(730)\Phi_u^{(2)}(\text{8c}) = 45 \text{ mGM}$; $\delta_u(780)\Phi_u^{(2)}(\text{8c}) = 35 \text{ mGM}$; $\delta_u(800)\Phi_u^{(2)}(\text{8c}) = 25 \text{ mGM}$. [f] $\delta_u(780)\Phi_u^{(2)}(\text{9c}) = 30 \text{ mGM}$; $\delta_u(800)\Phi_u^{(2)}(\text{9c}) = 20 \text{ mGM}$. [g] $\delta_u(780)\Phi_u^{(2)}(\text{10c}) = 40 \text{ mGM}$; $\delta_u(800)\Phi_u^{(2)}(\text{10c}) = 30 \text{ mGM}$.

stance, we calculated the same value for the rate constant for uncaging after one-photon excitation: $1.4 \pm 0.1 \times 10^{-3} \text{ min}^{-1}$ from both analyses in the case of **8c**. Table 2 displays the values of the action uncaging cross-section for one-photon excitation at $\lambda_{\text{exc}}^{(1)} = 325 \text{ nm}$ in the **nc** series, $\epsilon_u(325)\Phi_u^{(1)}(\text{nc})$. The larger variation in the signal in the irradiation experiments made analysis possible during even the slowest evolutions.

Irradiation experiments with two-photon excitation: Two approaches have been used already to determine the action uncaging cross-section for two-photon absorption, $\delta_u\Phi_u^{(2)}$. In the most general approach,^[7,8,43] the caged compound at a typical concentration of $100 \mu\text{M}$ is submitted continuously to the rather large power input (300–600 mW) of the focussed beam of a Ti:sapphire laser. Microliter aliquots from the irradiated solution are analyzed by HPLC as a function of time. The action uncaging cross-section for two-photon excitation of the caging group is eventually calculated from analysis of the release kinetics of the caged substrate after calibration of the laser pulse parameters by recording the fluorescence emission from a standard. The other approach is restricted to caged fluorescent compounds or to caged species that can be detected by using a fluorescent indicator.^[13,28] The measurements are typically performed at millimolar concentrations in caged compounds at an input laser power less than 100 mW. The latter approach relies on the analysis of the kinetic evolution, as well as of the steady-state value of the fluorescence intensity that arises from the focal volume illuminated by the beam. The action uncaging

cross-section for two-photon excitation of the caging group is derived from the dependence of the photolysis rate constant on the average laser power after calibration of the excitation volume with a fluorescence standard.

Here, we developed a new protocol to measure the action uncaging cross-section for two-photon excitation of fluorescent caged compounds. In principle, this is related to the second approach described above, however, here, fluorescence analysis is based on FCS after two-photon excitation.^[45–54] We observed and analyzed the large fluctuations in the fluorescence emission from the illuminated volume at the focus of a Ti:sapphire laser beam upon irradiation of a micromolar or submicromolar solution of a caged fluorescent compound. We computed the autocorrelation

function of fluorescence emission defined in Equation (1):

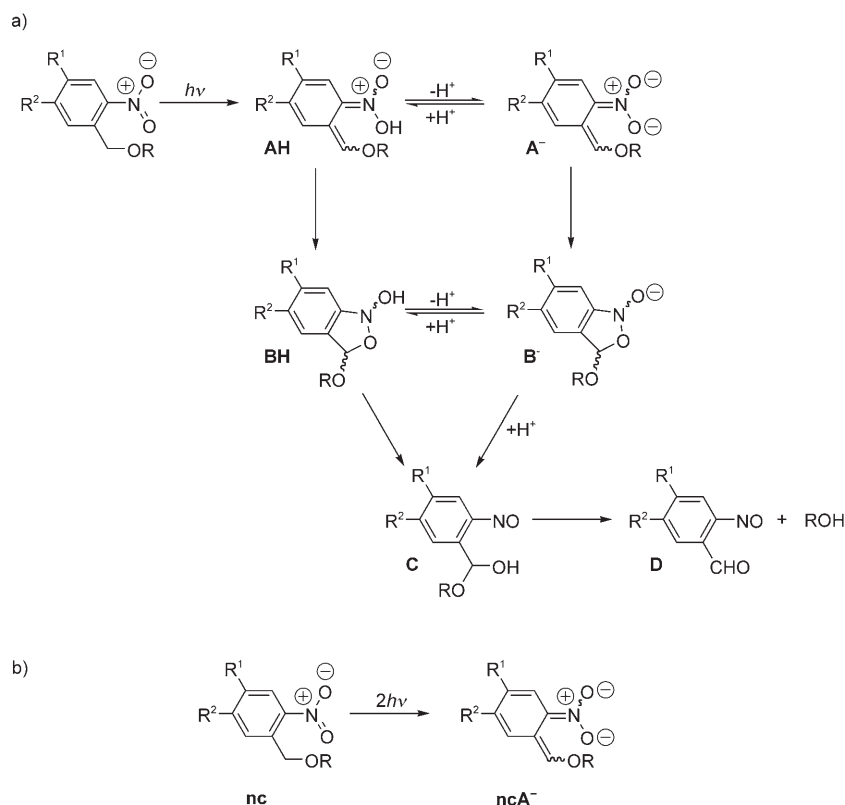
$$G\tau = \frac{\langle \delta n(\vec{r}, 0) \delta n(\vec{r}, \tau) \rangle}{n(\vec{r}) n(\vec{r})} \quad (1)$$

This gives the time-average of the products of the fluctuations of the number of photons $n(\vec{r}, t)$ collected from the illuminated volume, normalized by the product of the average number. In principle, $G(\tau)$ contains the desired kinetic information leading to $\delta_u\Phi_u^{(2)}$. In practice, $G(\tau)$ analysis is generally rather demanding in a reactive system that contains more than three reactants.^[45–47,55,56] In the present system, the FCS analysis is facilitated by 1) the limited kinetic window that is accessible by FCS after two-photon excitation and by 2) the knowledge of the mechanism/typical rate constants that are involved in releasing 2-nitrobenzyl caged compounds.

Both the temporal resolution of the autocorrelator and the characteristic diffusion time τ_D for a freely-moving fluorescent molecule to cross the focussed beam cause the kinetic window that can be accessed by FCS to be fixed.^[56] In the case of two-photon excitation of “small” molecules, such as the present caged compounds, kinetic information can be calculated typically within the 1–50 μs range. Thus, for the present purpose, one is interested in all events taking place within 50 μs after the primary photoreaction of the caged compounds.

The mechanism of uncaging of *ortho*-nitrobenzyl ethers that emerged from extensive studies is displayed in

Scheme 8a.^[24,25] For FCS analysis, the most significant information is that: 1) the primary photoreaction of 2-nitrobenzyl compounds provides aci-nitro tautomers **AH** within 5 ps; 2) **AH** ionization giving the basic state **A⁻** occurs above $pK_a(\text{AH/A}^-) \approx 4$ at a rate faster than $1 \times 10^6 \text{ s}^{-1}$; ^[25] 3) the formation of the acetal intermediate state **{BH, B⁻}** should not occur at a rate much faster than $1 \times 10^3 \text{ s}^{-1}$ at the pH of 9 that was used throughout the present experiments.^[25]



Scheme 8. a) Mechanism of uncaging of *ortho*-nitrobenzyl ethers, adapted from reference [25]; b) reduced mechanism that was used in this study to analyze the FCS data.

On the relevant timescale of analysis of the experimental autocorrelation function $G(\tau)$, the full mechanism displayed in Scheme 8a can be reduced consequently to the mechanism displayed in Scheme 8b: the caged species **nc** provides in a single step the basic state of the corresponding intermediate aci-nitro tautomers **ncA⁻**. In addition, one anticipates that conversion of the excited molecules of caged compound leading to photolysis is complete within 1 μs . In principle, the present illuminated reactive system should behave as a nonreactive mixture of two fluorescent species, **nc** and **ncA⁻**, upon observation by FCS after two-photon excitation. Under such conditions, $\delta_u \Phi_u^{(2)}$ can be calculated, as explained in the Experimental Section, from the dependence on the laser power input of the **ncA⁻/nc** proportions in the illuminated volume.

Figure 4a displays typical experimental FCS autocorrelation functions $G(\tau)$ that were recorded on a 1 μM **10c** solu-

tion in $\text{CH}_3\text{CN}/20 \text{ mM}$ Tris pH 9 buffer 1:1 (v/v) that was submitted to increasing input-laser powers. Throughout this study, we always obtained satisfactory fits of the experimental points by using Equation (14) that is associated with a nonreactive mixture of two fluorescent species. As anticipated from the similar sizes of the caged derivatives and the released substrates, the calculated diffusion times τ_D were essentially independent of laser powers below 15 mW at the sample level. In addition, they were in line with expectations. For instance, we calculated $\tau_D = 27 \pm 5 \mu\text{s}$ for **10c**. In fact, we obtained typically $\tau_D = 25 \mu\text{s}$ in a similar solvent for a closely related molecule.^[56]

Information regarding the composition of the **ncA⁻/nc** mixture that leads to $\delta_u \Phi_u^{(2)}$ is contained in the $G(0)$ value in the FCS autocorrelation curve. A typical example of dependence of $G(0)$ on the laser power at the sample is shown in Scheme 8b. The experimental points can be fitted satisfactorily with Equation (15) that originates from the theoretical derivation by using the mechanism shown in Scheme 8b (see Experimental Section). In the case of **10c** at $\lambda_{\text{exc}}^{(2)} = 750 \text{ nm}$, the fit provides a relative brightness of **10cA⁻** to **10c** of 2500 ± 200 , and $\delta_u \Phi_u^{(2)} = 0.04 \text{ GM}$ for the uncaging cross-section for two-photon excitation. Table 2 summarizes the corresponding parameter values that were measured for the series of caged coumarins investigated.

Discussion

We first evaluated whether choosing caged substrates that absorb light within the range of the excitation wavelength for uncaging 1) perturbs the analyses of the measured action uncaging cross-sections to calculate the corresponding quantum yields of uncaging and 2) makes the latter representative of uncaging quantum yields even if the caged substrate is nonabsorbing. Two different issues must be addressed. Firstly, one has to examine whether it is only the light that is absorbed by the *o*-nitrobenzyl moiety that leads to uncaging. Secondly, one must evaluate whether supplementary relaxation pathways may compete with the photo-release of the caged substrate after light absorption by the *o*-nitrobenzyl chromophore due to the presence of another chromophore within the caged substrate.

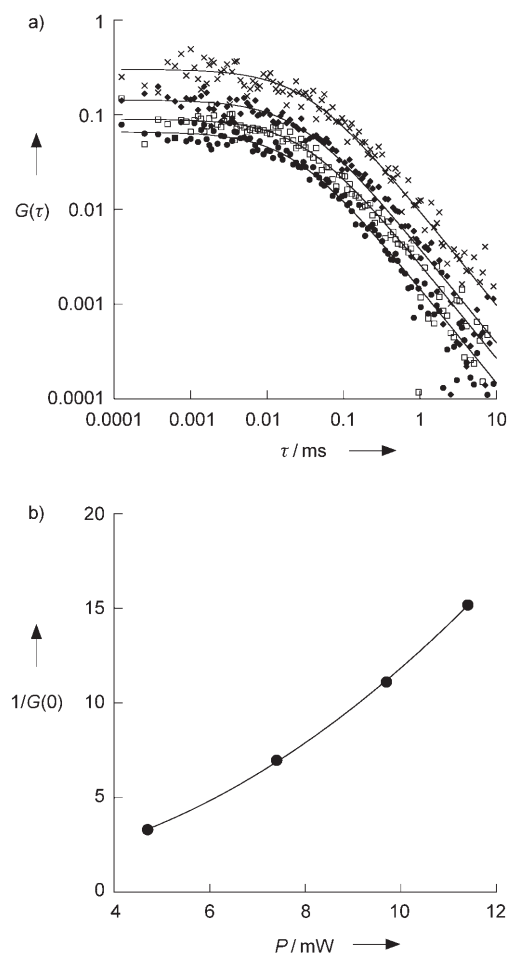


Figure 4. a) FCS autocorrelation curves $G(\tau)$ recorded at 293 K from 1 μM **10c** solutions at increasing laser powers at the sample, P ($P=5$ mW, \times ; $P=7.5$ mW, \blacklozenge ; $P=10$ mW, \square ; $P=11.5$ mW, \bullet ; $\lambda_{\text{exc}}^{(2)}=750$ nm). Fitting the experimental points by using Equation (14) gave 32 ± 3 μs ($P=5$ mW), 27 ± 3 μs ($P=7.5$ mW), 28 ± 3 μs ($P=10$ mW), and 22 ± 3 μs ($P=11.5$ mW) for the diffusion times τ_D . b) Dependence of $1/G(0)$ as a function of P . Symbols: experimental data; line: fit according to Equation (15). From this curve, $\alpha=2500 \pm 200$ and $\delta_u(750)\Phi_u^{(2)}=40$ mGM.

We did not observe any strong coupling between the chromophores that are contained in the *o*-nitrobenzyl protecting groups and in the caged substrates in the **nb** and **nc** series. This suggests that the corresponding chromophores behave essentially independently with regards to light absorption.^[42] In contrast, energy transfer can occur towards the chromophore absorbing at the largest wavelength after excitation of the chromophore absorbing at the lowest wavelength.^[57] Such a process may be significant in calculating the quantum yield of uncaging after one-photon excitation $\Phi_u^{(1)}$ from the corresponding action uncaging cross-section for one-photon excitation $\epsilon_u(325)\Phi_u^{(1)}$ at $\lambda_{\text{exc}}^{(1)}=325$ nm if the *o*-nitrobenzyl chromophore absorbs at the largest wavelength. If energy transfer from the excited state of the caged substrate to the *o*-nitrobenzyl moiety is faster than its relaxation, one should

take the molar absorption coefficient of the caged compound to calculate $\Phi_u^{(1)}$. In the opposite case, one should use the molar absorption coefficient of the *o*-nitrobenzyl moiety.

In the **nc** series, energy transfer cannot occur from the coumarin to the *o*-nitrobenzyl moiety because the former always absorbs light at a larger wavelength than the latter. In contrast, energy transfer could be relevant in most **nb** caged compounds (except **1b** and possibly **3b**). In view of the very low quantum yields of fluorescence emission of nitrobenzene derivatives, such as **3a**, that would slow considerably any energy transfer by the Förster mechanism to the *o*-nitrobenzyl moiety,^[57] we did not consider energy transfer in calculating $\Phi_u^{(1)}$ in the data analysis.^[58] Thus, we used the molar absorption coefficients of the alcohols **na** as appropriate orders of magnitude of the corresponding molar absorption coefficients of alkyl ethers of the *o*-nitrobenzyl moieties. In fact, choosing the molar absorption coefficient of the caged compound **nb** would not change considerably the $\Phi_u^{(1)}$ values, except for **1b**. Indeed, at the one-photon excitation wavelength that was used in the present series of experiments ($\lambda_{\text{exc}}^{(1)}=325$ nm), the molar absorption coefficients of an alkyl ether of *p*-nitrophenol, such as **3a**, is about $7 \times 10^3 \text{ M}^{-1} \text{ cm}^{-1}$ and this value is lower than the molar absorption coefficients of the *o*-nitrobenzyl moieties that were investigated in the present study.

Table 2 displays the results. We first examined the significance of the backbone conjugated to the nitro substituent if the benzylic position bears two hydrogen atoms. In the **nb** series, the quantum yield for uncaging after one-photon excitation is largest for **1b**, with $\Phi_u^{(1)}(\mathbf{1b}) \approx 10\%$. $\Phi_u^{(1)}(\mathbf{nb})$ values are within the 1% range for **3b**, **4b**, **7b**, and **8b**. In particular, $\Phi_u^{(1)}(\mathbf{4b})$ compares satisfactorily with the reported value of a phenol caged with the **4** backbone.^[43] Uncaging was too slow for **5b**, **6b**, and **9b** to calculate the corresponding quantum yields reliably. In fact, $\Phi_u^{(1)}$ seems to drop as the maximum wavelength of absorption of the *o*-nitro protecting group increases. This trend was already observed upon going from the 2-nitrobenzyl to the 4,5-dimethoxy-2-nitrobenzyl group.^[7] It was also implicit in reported results,^[29] but the absence of measurements of $\Phi_u^{(1)}$ in the latter work makes the comparison difficult. We observed a similar trend in the **nc** series. Interestingly, $\Phi_u^{(1)}(\mathbf{4c})$ is in line with reported values of the quantum yields of uncaging after one-photon excitation for **4**-caged nonabsorbing carboxylic acids.^[7] In fact, energy transfer could occur from the **4** *o*-nitrobenzyl moiety to the coumarin before the primary photoreaction leading to aci-nitro tautomers (Scheme 8a). Under such conditions, we should observe lower quantum yields of uncaging in our series than with nonabsorbing caged carboxylic acids. The absence of any energy transfer probably results from the very low quantum yields of fluorescence emission from the *o*-nitrobenzene derivatives that slows energy transfer by the Förster mechanism, and from the fast subpicosecond timescale that was reported for the primary photoreaction.^[25] All together, the present observations suggest that the photophysical properties of the caged substrate do not alter strongly the uncaging behavior with

regard to the *o*-nitrobenzyl photochemistry. In fact, such a result is fortunate because evaluation of the uncaging efficiency upon two-photon excitation is facilitated greatly if use is made of fluorescent caged probes. In addition, it allows us to use typical values of the uncaging quantum yields to evaluate the uncaging quantum yields of caged fluorophores that are often used as fluorescent polar tracers in biology.

The significance of introducing a substituent on the benzylic position is based on the results obtained in the **4c** series. The effect is significant, but it remains weak: the best tribromomethyl substituent exhibits a quantum yield for uncaging after one-photon excitation that is only four times larger than that of the cyano substituent that gives the worst results here. Analysis of these observations is difficult. In fact, the benzylic substituent can introduce different types of alterations governing the efficiency of the uncaging pathway after light absorption by the caged compound. Electronic effects should affect the lability of the benzylic proton that is involved in the uncaging mechanism (Scheme 8a). The presence of heavy atoms could promote alternative relaxation pathways implying the triplet states. Eventually, steric hindrance could also play a role. In particular, we did not obtain the favorable results reported with the trifluoromethyl as well as with the cyano substituents.^[10,30] The corresponding discrepancy questions the use of the benzylic substituent to improve quantum yields of uncaging after one-photon excitation; efficiencies could be strongly dependent on the nature of the caged substrate.

We used the quantum yields for uncaging after one-photon excitation of the **nb** series and the molar absorption coefficients of the **na** alcohols to derive a representative order of magnitude of the action uncaging cross-section of the present *o*-nitrobenzyl photolabile protecting groups (Table 2). In fact, the protecting groups **7** and **8** appear better than the reference **4** at $\lambda_{\text{exc}}^{(1)} = 350$ nm. The results obtained in the **4c** series probably indicate that **4Cl** and **4Br** would also be more efficient than **4**. Despite such improvements, one can notice that the action uncaging cross-section for one-photon excitation in the present series should be increased by hardly more than one order of magnitude by combining the best conjugated backbone and benzylic substituent.

We now turn to the results obtained from two-photon excitation. The action uncaging cross-section for two-photon excitation of the 4,5-dimethoxy-2-nitrobenzyl photolabile protecting group has been already measured by two different methods for nonabsorbing caged carboxylic acids: $\delta_u(740)\Phi_u^{(2)} = 0.03$ GM^[7] and $\delta_u(740)\Phi_u^{(2)} = 0.01$ GM^[28] were reported, respectively. Here, we derived $\delta_u(740)\Phi_u^{(2)} = 0.02$ GM for **4c**. In fact, this fair agreement led us to the same conclusion independently of the excitation mode: in the **nc** series, the energy transfer from the *o*-nitrobenzyl moiety to the coumarin is not competing considerably with the primary photoreaction leading to substrate release.

We first consider the $\delta_u(750, \text{nc})\Phi_u^{(2)}$ values given in Table 2 by investigating the role of the backbone conjugated

to the nitro substituent if the benzylic position bears two hydrogen atoms. In fact, we obtained essentially similar values, whatever the structure of the conjugated backbone in the present series: $\delta_u(750)\Phi_u^{(2)}$ for **4c**, **5c**, **8c**, **9c**, and **10c** are all within the 0.02–0.05 GM range. A similar conclusion arises at 800 nm: $\delta_u(800)\Phi_u^{(2)}$ lies between 0.02 and 0.03 GM for **8c**, **9c**, and **10c** whereas 0.01 GM was reported for a 4,5-dimethoxy-2-nitrobenzyl derivative at the same excitation wavelength.^[7]

Figure 1 displays parts of the uncaging absorption spectra upon two-photon excitation $\delta_u\Phi_u^{(2)}$ for **8c**, **9c**, and **10c**. In line with the corresponding results that were reported for 4,5-dimethoxy-2-nitrobenzyl caged compounds,^[7,28] they reasonably compare with the absorption spectra upon one-photon excitation after dividing the excitation wavelength by a factor two. The whole collection of results suggests that the same excited state is involved in photolysis after both one- and two-photon excitation in the *o*-nitrobenzyl series. Consequently, if it is assumed that the quantum yields of uncaging after one- and two-photon excitation are identical, that is, $\Phi_u^{(1)} = \Phi_u^{(2)}$, the data contained in Table 2 can be used to derive orders of magnitude for the two-photon absorption cross-sections of the *o*-nitrobenzyl moieties by the expression: $\delta(\lambda_{\text{exc}}^{(2)}) = \delta_u(\lambda_{\text{exc}}^{(2)})\Phi_u^{(2)}/\Phi_u^{(1)}$. Thus, we derived $\delta(750, \text{4c}) \approx 3$ GM and $\delta(750, \text{nc}) \approx 20$ –50 GM (**n** = **8**, **9**, and **10**). The value of $\delta(750, \text{4c})$ confirms that the coumarin chromophores do not contribute strongly, if at all, to light absorption leading to uncaging because one would typically expect $\delta(750, \text{12}) \approx 10$ –20 GM for the coumarin **12**.^[31] In addition, these estimates are in reasonable agreement with the expectations based on molecular structure. For instance, we recorded fluorescence excitation spectra for two-photon excitation to measure $\delta(\lambda_{\text{max}}^{(2)}) \approx 60$ GM in a series that is closely related to the *o*-nitrobenzyl chromophore in **10c** that should here exhibit $\delta(\lambda_{\text{max}}^{(2)}) \approx 40$ GM.^[59,60]

The role of the benzylic substituent can be analyzed in the **4c** series. We observed $\delta_u(750, \text{4cBr})\Phi_u^{(2)} > \delta_u(750, \text{4cCl})\Phi_u^{(2)} \approx \delta_u(750, \text{4cCN})\Phi_u^{(2)} \approx \delta_u(750, \text{4c})\Phi_u^{(2)} > \delta_u(750, \text{4cF})\Phi_u^{(2)}$. This trend seems reasonable if it is assumed again that uncaging cross-sections for one- and two-photon excitation are identical. In fact, all the members of the **4c** series share the same *o*-nitrobenzyl chromophore and should consequently exhibit the same $\delta(750)$ value. Then, the evolution of $\delta_u(750)\Phi_u^{(2)}$ and $\Phi_u^{(1)}$ would be comparable, which is indeed essentially observed. The best benzylic substituent is again tribromomethyl, which exhibits a quantum yield for uncaging after two-photon excitation that is three times larger than that for any other substituent.

Despite the expected increase in the action uncaging cross-section for two-photon excitation that would result from the appropriate choice of the best present *o*-nitrobenzyl backbone and benzylic substituent, we reach again a conclusion similar to the one upon using one-photon excitation: the action uncaging cross-section for two-photon excitation should be increased by hardly more than one order of magnitude in the *o*-nitrobenzyl series.

Conclusion

We evaluated the *o*-nitrobenzyl platform for designing photolabile protecting groups with red-shifted absorption that could be photolyzed upon one- and two-photon excitation. Special attention was paid to the latter excitation mode in view of promising biological applications.

From the synthetic point of view, this work shows that several strategies can be envisaged to introduce the 2-nitrobenzyl motif in putative photolabile protecting groups. We generated several 2-nitrobenzyl alcohols and the corresponding synthetic pathways could be transposed easily to yield other 2-nitrobenzyl derivatives. In particular, the palladium-coupling approach relying on the **IIa** synthon opens the way to the syntheses of other conjugated species.

As anticipated from the availability of reliable structure–property relationships, the 2-nitrobenzyl alcohols synthesized in the present study exhibit absorption properties in agreement with expectations based on their molecular structures. In particular, we improved considerably the match between their absorption features and the wavelength ranges of the current laser sources for two-photon excitation. With regard to the 4,5-dimethoxy-2-nitrobenzyl reference, several of the 2-nitrobenzyl photolabile protecting groups described possess significantly red-shifted and enlarged light absorption upon one- or two-photon excitation. We anticipate that better results could be obtained with more conjugated backbones that could exhibit more red-shifted and larger light absorptions than those in the present series.

In addition to the cross-sections for light absorption, the quantum yields of uncaging after one- and two-photon excitation are the other significant photophysical parameters that determine the values of the action uncaging cross-sections. We showed that the caged substrates were released cleanly upon photolysis in the whole series investigated. With appropriate caged substrates from the present series, the action uncaging cross-sections can be derived easily and reliably from experiments based on UV-visible absorption and fluorescence emission (one-photon excitation) and from FCS (two-photon excitation). For the purpose of molecular engineering, our observations suggest that the values of the quantum yields of uncaging after one- and two-photon excitation are similar in the 2-nitrobenzyl series. This observation should facilitate the design of future photolabile protecting groups bearing a donor–acceptor backbone. Indeed, most available quantum yields of uncaging rely presently on one-photon excitation.

We found that the quantum yields of uncaging remained low in the whole 2-nitrobenzyl series investigated: they generally lie within the 0.1–1 % range. This is a drawback to enlarging the action uncaging cross-sections for one- and two-photon excitation. For instance, cross-sections for two-photon absorption that are ten times larger than in the present series would be required to get results comparable with those of the best available series. Moreover, we observed that the quantum yields of uncaging dropped if the maximum of wavelength absorption of the *o*-nitrobenzyl moiety

was increased. Although difficult to analyze at the present time, this result indicates that one cannot necessarily optimize independently both the absorption and the uncaging properties of a photolabile protecting group. In the 2-nitrobenzyl series, the observed trend could make it difficult to enlarge the action uncaging cross-sections beyond the existing values.

Experimental Section

Syntheses: The syntheses of the final compounds, as well as of the synthetic intermediates, are detailed in the Supporting Information.

UV/Vis absorption: UV/Vis absorption spectra were recorded at 293 K by using a Kontron Uvikon-940 spectrophotometer. Molar absorption coefficients were calculated by checking the validity of the Beer–Lambert law.

Steady-state fluorescence emission: Corrected fluorescence spectra were obtained by using a Photon Technology International LPS 220 spectrofluorometer. Solutions for fluorescence measurements were adjusted to concentrations so that the absorption maximum was around 0.15 at the excitation wavelength (typical range: a few micromolar). The overall fluorescence quantum yields after one-photon excitation $\Phi_F^{(1)}$ were calculated from Equation (2):

$$\Phi_F^{(1)} = \Phi_{\text{ref}}^{(1)} \frac{1 - 10^{-A_{\text{ref}}(\lambda_{\text{exc}})}}{1 - 10^{-A(\lambda_{\text{exc}})}} \frac{D}{D_{\text{ref}}} \left(\frac{n}{n_{\text{ref}}} \right)^2 \quad (2)$$

in which the subscript “ref” stands for standard samples, $A(\lambda_{\text{exc}})$ is the absorbance at the excitation wavelength, D is the integrated emission spectrum, and n is the refractive index for the solvent. The error in the experimental value of $\Phi_F^{(1)}$ was estimated to be $\pm 10\%$. The standard fluorophore for the quantum yields measurements was quinine sulfate in 0.1 M H_2SO_4 with $\Phi_{\text{ref}}^{(1)} = 0.55$.^[62]

Irradiation experiments: Irradiation experiments were performed at 20 °C in $\text{CH}_3\text{CN}/20\text{ mM Tris pH 9 buffer 1:1 (v/v)}$. No thermal hydrolysis was observed on the timescale of the present irradiation experiments (24 h).

One-photon excitation: Irradiations relying on one-photon excitation were performed at 325 nm on 3 mL samples in $1 \times 1\text{ cm}^2$ quartz fluorescence cuvettes under constant stirring. Excitations were performed by using the 75 W xenon lamp of a Photon Technology International LPS 220 spectrofluorometer at several slit widths. The corresponding incident-light intensities were systematically calibrated by determining the kinetics of photoconversion of the α -(4-dimethylaminophenyl)-*N*-phenylnitrone into 3-(4-dimethylaminophenyl)-2-phenyloxaziridine in fresh dioxane as described in reference [44]. For the present series of experiments, typical incident-light intensities were within the $1 \times 10^{-4}\text{ Einstein min}^{-1}$ range.

To derive the cross-section for uncaging after one-photon excitation, we considered that the illuminated system was submitted to the reaction:



in which ROPG, ROH, and PG designate the caged species, the species that was initially caged, and the product from the protecting moiety after ROH release.

The reaction rate for photodeprotection of the caged compound ROPG is proportional to the intensity of the monochromatic excitation light absorbed by ROPG at the excitation wavelength that leads to uncaging, $I_u(\lambda_{\text{exc}}^{(1)})$, and to the uncaging cross-section for one-photon excitation, $\Phi_u^{(1)}$:

$$-\frac{d[\text{ROPG}]}{dt} = \frac{I_u(\lambda_{\text{exc}}^{(1)})\Phi_u^{(1)}}{V} \quad (4)$$

in which V is the irradiated volume. $I_u(\lambda_{\text{exc}}^{(1)})$ and all the subsequent absorbed-light intensities are expressed in Einstein per unit of time. By introducing $A_u(\lambda_{\text{exc}}^{(1)})$, $A_{\text{tot}}(\lambda_{\text{exc}}^{(1)})$, and $I_0(\lambda_{\text{exc}}^{(1)})$ that designate the effective ROPG absorbance for uncaging, the total absorbance, and the intensity of the incident beam at the excitation wavelength, respectively, Equation (4) provides the following:

$$-\frac{d[\text{ROPG}]}{dt} = \frac{1 - \exp[-2.3A_{\text{tot}}(\lambda_{\text{exc}}^{(1)})] \Phi_u^{(1)} I_0(\lambda_{\text{exc}}^{(1)})}{A_{\text{tot}}(\lambda_{\text{exc}}^{(1)})} A_u(\lambda_{\text{exc}}^{(1)}) \quad (5)$$

If $A_{\text{tot}}(\lambda_{\text{exc}}^{(1)}) \ll 1$, one obtains at first order:

$$-\frac{d[\text{ROPG}]}{dt} = k[\text{ROPG}] \quad (6)$$

with

$$k = \frac{2.3\Phi_u^{(1)} I_0(\lambda_{\text{exc}}^{(1)}) \varepsilon_u(\lambda_{\text{exc}}^{(1)}) l}{V} \quad (7)$$

in which $\varepsilon_u(\lambda_{\text{exc}}^{(1)})$ and l represent the effective molar absorption coefficient for uncaging of ROPG at the excitation wavelength, and the pathlength of the light beam, respectively.

By assuming that the system contains initially only ROPG, one then easily derives:

$$\frac{A_{\text{tot}}(\lambda_{\text{exc}}^{(1)}, t)}{A_{\text{tot}}(\lambda_{\text{exc}}^{(1)}, 0)} = \frac{\varepsilon_{\text{ROH}}(\lambda_{\text{exc}}^{(1)}) + \varepsilon_{\text{PG}}(\lambda_{\text{exc}}^{(1)})}{\varepsilon_{\text{ROPG}}(\lambda_{\text{exc}}^{(1)})} + \left(1 - \frac{\varepsilon_{\text{ROH}}(\lambda_{\text{exc}}^{(1)}) + \varepsilon_{\text{PG}}(\lambda_{\text{exc}}^{(1)})}{\varepsilon_{\text{ROPG}}(\lambda_{\text{exc}}^{(1)})}\right) \exp(-kt) \quad (8)$$

in which ε_{ROH} , ε_{PG} , and $\varepsilon_{\text{ROPG}}$ designate the molar absorption coefficients of ROH, PG, and ROPG, respectively.

For the present series of experiments, the total absorbance at the excitation wavelength had a maximum of around 0.15 to avoid the effects associated with inner filtering and to be in the region of approximation leading to Equation (6). Under the same experimental conditions, the temporal evolution of the intensity $I_F(\lambda_{\text{exc}}^{(1)}, \lambda_{\text{em}})$ of the steady-state fluorescence emission at $\lambda_{\text{exc}}^{(1)}$ upon excitation at λ_{em} can be written:

$$\frac{I_F(\lambda_{\text{exc}}^{(1)}, \lambda_{\text{em}}, t)}{I_F(\lambda_{\text{exc}}^{(1)}, \lambda_{\text{em}}, 0)} = \frac{Q_{\text{ROH}}^{(1)}(\lambda_{\text{exc}}^{(1)}) + Q_{\text{PG}}^{(1)}(\lambda_{\text{exc}}^{(1)})}{Q_{\text{ROPG}}^{(1)}(\lambda_{\text{exc}}^{(1)})} + \left(1 - \frac{Q_{\text{ROH}}^{(1)}(\lambda_{\text{exc}}^{(1)}) + Q_{\text{PG}}^{(1)}(\lambda_{\text{exc}}^{(1)})}{Q_{\text{ROPG}}^{(1)}(\lambda_{\text{exc}}^{(1)})}\right) \exp(-kt) \quad (9)$$

in which $Q_x^{(1)} = \varepsilon_x(\lambda_{\text{exc}}^{(1)}) \Phi_F^{(1)}(x)$ designates the brightness after one-photon excitation of ROH, PG, and ROPG ($\Phi_F^{(1)}(x)$ is the quantum yield of fluorescence emission after one-photon excitation of the species x).

Two-photon excitation: Our home-built two-photon excitation FCS setup has been previously reported.^[56,63] Illumination is provided by a mode-locked titanium-sapphire laser (Mira pumped by Verdi, Coherent) through a 60 \times , 1.2 NA water immersion objective (Olympus). The sample at 1 μM concentration was contained in a cuvette described in reference [56]. To measure excitation power, we measured the input-laser power by using a Lasermate powermeter (Coherent) and the power loss between input and sample level. Power at the sample level was then derived without disturbing the cuvette. For the present series of experiments, fluorescence photons were collected through a 560/80 nm band-pass filter with two avalanche photodiodes (APD, SPCM-AQR-14, Perkin-Elmer, Vaudreuil, Canada) coupled to an ALV-6000 correlator (ALV GmbH). At 0.1–5 μM concentrations in caged coumarin, we typically observed signals of 500 Hz to 10 kHz on each APD. We investigated the dependence of the fluorescence emission from **12** as a function of the excitation power. The range of investigated excitation powers was chosen to be in the region of power-squared dependence for the intensity of fluorescence emission (21–85 mW input-laser power, which corresponds to 3–12 mW at the sample level). Under these experimental conditions, no contribution of the triplet state to the experimental FCS autocorrelation curves was observed. In the present work, a typical FCS experiment con-

sisted of between several hundred and a few thousand acquisitions of three seconds each, leading to a typical acquisition time of 1 h.

The experimental FCS autocorrelation curves $G(\tau)$ defined in Equation (1) were fitted by assuming that the solution contained two freely diffusing species with the same diffusion constant D , **nc** and **ncA**[−] (Scheme 8b). By denoting these species as **1** and **2**, respectively, the associated fitting function is:^[53]

$$G(\tau) = \frac{(Q_1^{(2)})^2 N_1 + (Q_2^{(2)})^2 N_2}{[Q_1^{(2)} N_1 + Q_2^{(2)} N_2]^2} \frac{1}{1 + \tau/\tau_D} \quad (10)$$

In Equation (10), $Q_1^{(2)}$ and $Q_2^{(2)}$ designate the respective brightnesses of **1** and **2** ($Q_x^{(2)} = \delta_x \Phi_{F,x}^{(2)}$ in which δ_x designates the cross-section for two-photon absorption of **x** and $\Phi_{F,x}^{(2)}$ is the quantum yield of fluorescence of **x** after two-photon excitation), N_1 and N_2 represent the number of molecules of **1** and **2** in the illuminated spot described as two-dimensional Gaussian, and τ_D is the diffusion time of **1** and **2** through the beam waist. By introducing the relative brightness $\alpha = Q_2^{(2)}/Q_1^{(2)}$, Equation (10) becomes:

$$G(\tau) = \frac{N_1 + \alpha^2 N_2}{(N_1 + \alpha N_2)^2} \frac{1}{1 + \tau/\tau_D} \quad (11)$$

Provided that α is large enough, the amplitude of the FCS autocorrelation curve can reveal the presence of even a very small amount of **2**, N_2 . By following the theoretical treatment of Kiskin et al.,^[13] the averaged number of molecules of **2** in the illuminated spot in the steady state equals:

$$\frac{N_2}{N_{\text{tot}}} \approx \frac{k\tau_D/2.5}{1 + k\tau_D/2.5} \quad (12)$$

in which $N_{\text{tot}} = N_1 + N_2$ and:

$$k = 1.17 \delta_u \Phi_u^{(2)} \frac{T}{\tau_p} \left(\frac{\lambda}{\pi h c w_0^2} \right)^2 P^2 V F \quad (13)$$

In Equation (13), δ_u is the cross-section for two-photon absorption leading to uncaging at the excitation wavelength $\lambda_{\text{exc}}^{(2)}$, $\Phi_u^{(2)}$ is the quantum yield of uncaging after two-photon excitation, T is the period of the laser pulses (13.6 ns in our case), τ_p (200 fs) is the duration of the laser pulses, w_0 (0.3 μm) is the waist of the focussed laser beam, P is the laser power at the sample and $V F$ is a geometrical term (equal to 0.63 if $w_0 > 0.3 \mu\text{m}$, like in the present case).

Preliminary results suggested that $\frac{N_2}{N_1} \ll 1$ and $\alpha \gg 1$. Thus, we considered the approximate correlation function [Eq. (14)] with fewer undetermined constants to fit experimental data:

$$G(\tau) = \frac{N_{\text{tot}} + \alpha^2 N_2}{(N_{\text{tot}} + \alpha N_2)^2} \frac{1}{1 + \tau/\tau_D} \quad (14)$$

In the fitting process using Equation (14), N_{tot} was assumed from the concentration used in **nc** and of the illuminated volume from a preliminary calibration,^[56] and only $\frac{N_{\text{tot}} + \alpha^2 N_2}{(N_{\text{tot}} + \alpha N_2)^2}$ and τ_D were adjusted. By writing $k = \gamma P^2$ and $\beta = \tau_D \gamma / 2.5$, and by considering that $\beta P^2 \ll 1$ under the present experimental conditions, one obtains:

$$\frac{1}{G(0)} \approx N_{\text{tot}} \frac{(1 + \alpha \beta P^2)^2}{1 + \alpha^2 \beta P^2} \quad (15)$$

FCS autocorrelation curves were recorded at different laser powers P . The curves were fitted by using Equation (14) to calculate $G(0)$ and τ_D (data were processed by using Matlab and Origin softwares). The values of $1/G(0)$ were then plotted as a function of P and the experimental data were fitted by using Equation (15) to calculate the values of α and β .^[64] The action uncaging cross-section for two-photon excitation $\delta_u \Phi_u^{(2)}$ was finally derived from the β value.

Acknowledgements

Dr. J.-F. Allemand is gratefully acknowledged for his help to design FCS experiments. This research was financially supported by the "Association pour la Recherche sur le Cancer" (ARC) (2005, project no. 3787).

- [1] V. N. R. Pillai, *Synthesis* **1980**, 1–26.
- [2] C. G. Bochet, *J. Chem. Soc. Perkin Trans. 1* **2002**, 125–142.
- [3] A. P. Pelliccioli, J. Wirz, *Photochem. Photobiol. Sci.* **2002**, *1*, 441–458.
- [4] H. Ando, T. Furuta, R. Y. Tsien, H. Okamoto, *Nat. Genet.* **2001**, *28*, 317–325.
- [5] R. Wieboldt, K. R. Gee, L. Niu, D. Ramesh, B. K. Carpenter, G. P. Hess, *Proc. Natl. Acad. Sci. USA* **1994**, *91*, 8752–8756.
- [6] N. A. Porter, J. W. Thuring, H. Li, *J. Am. Chem. Soc.* **1999**, *121*, 7716–7717.
- [7] T. Furuta, S. S.-H. Wang, J. L. Dantzker, T. M. Dore, W. J. Bybee, E. M. Callaway, W. Denk, R. Y. Tsien, *Proc. Natl. Acad. Sci. USA* **1999**, *96*, 1193–2000.
- [8] O. D. Fedoryak, T. M. Dore, *Org. Lett.* **2002**, *4*, 3419–3422.
- [9] A. Banerjee, C. Grever, L. Ramakrishnan, J. Jäger, A. Gameiro, H.-G. A. Breiter, K. R. Gee, B. K. Carpenter, G. P. Hess, *J. Org. Chem.* **2003**, *68*, 8361–8367.
- [10] A. Specht, M. Goeldner, *Angew. Chem.* **2004**, *116*, 2042–2046; *Angew. Chem. Int. Ed.* **2004**, *43*, 2008–2012.
- [11] M. Lukeman, J. C. Scaiano, *J. Am. Chem. Soc.* **2005**, *127*, 7698–7699.
- [12] O. D. Fedoryak, J.-Y. Sul, P. G. Haydon, G. C. R. Ellis-Davies, *Chem. Commun.* **2005**, 3664–3666.
- [13] N. Kiskin, R. Chillingworth, J. A. McCray, D. Piston, D. Ogden, *Eur. Biophys. J.* **2002**, *30*, 588–604.
- [14] M. Lu, O. D. Fedoryak, B. R. Moister, T. M. Dore, *Org. Lett.* **2003**, *5*, 2119–2122.
- [15] M. Albota, D. Beljonne, J.-L. Brédas, J. E. Ehrlich, J.-Y. Fu, A. A. Heikal, S. E. Hess, T. Kogej, M. D. Levin, S. R. Marder, D. McCord-Maughon, J. W. Perry, H. Röckel, M. Rumi, G. Subramanian, W. W. Webb, X.-L. Wu, C. Xu, *Science* **1998**, *281*, 1653–1656.
- [16] C. Le Droumaguet, O. Mongin, M. H. V. Werts, M. Blanchard-Desce, *Chem. Commun.* **2005**, 2802–2804.
- [17] R. Jasuja, J. Keyoung, G. P. Reid, D. R. Trentham, S. Khan, *Biophys. J.* **1999**, *76*, 1706–1719.
- [18] F. G. Cruz, J. T. Koh, K. H. Link, *J. Am. Chem. Soc.* **2000**, *122*, 8777–8778.
- [19] A. Barth, J. E. T. Corrie, *Biophys. J.* **2002**, *83*, 2864–2871.
- [20] Q. Cheng, M. G. Steinmetz, V. Jayaraman, *J. Am. Chem. Soc.* **2002**, *124*, 7676–7677.
- [21] M. Ghosh, I. Ichetovkin, X. Song, J. S. Condeelis, D. S. Lawrence, *J. Am. Chem. Soc.* **2002**, *124*, 2440–2441.
- [22] W. F. Veldhuyzen, Q. Nguyen, G. McMaster, D. S. Lawrence, *J. Am. Chem. Soc.* **2003**, *125*, 13358–13359.
- [23] S. Abbruzzetti, S. Sottini, C. Viappiani, J. E. T. Corrie, *J. Am. Chem. Soc.* **2005**, *127*, 9865–9874.
- [24] J. E. T. Corrie, A. Barth, V. R. N. Munasinghe, D. R. Trentham, M. C. Hutter, *J. Am. Chem. Soc.* **2003**, *125*, 8546–8554.
- [25] Y. V. Il'ichev, M. A. Schwörer, J. Wirz, *J. Am. Chem. Soc.* **2004**, *126*, 4581–4595.
- [26] B. Hellrung, Y. Kamdzhilov, M. Schwörer, J. Wirz, *J. Am. Chem. Soc.* **2005**, *127*, 8934–8935.
- [27] Y. V. Il'ichev, *J. Phys. Chem. A* **2003**, *107*, 10159–10170.
- [28] E. B. Brown, J. B. Shear, S. R. Adams, R. Y. Tsien, W. W. Webb, *Biophys. J.* **1999**, *76*, 489–499.
- [29] C. G. Bochet, *Tetrahedron Lett.* **2000**, *41*, 6341–6346.
- [30] M. C. Pirrung, W. H. Pieper, K. P. Kaliappan, M. R. Dhananjayan, *Proc. Natl. Acad. Sci. USA* **2003**, *100*, 12548–12553.
- [31] C. Xu, W. W. Webb, *J. Opt. Soc. Am. B* **1996**, *13*, 481–491.
- [32] E. Cogné-Laage, J.-F. Allemand, O. Ruel, J.-B. Baudin, V. Croquette, M. Blanchard-Desce, L. Jullien, *Chem. Eur. J.* **2004**, *10*, 1445–1455.
- [33] N. M. Yoon, C. S. Pak, H. C. Brown, S. Krishnamurthy, T. P. Stocky, *J. Org. Chem.* **1973**, *38*, 2786–2792.
- [34] M. C. Venuti, G. H. Jones, R. A. Alvarez, J. J. Bruno, *J. Med. Chem.* **1987**, *30*, 303–318.
- [35] G. V. De Lucca, U. T. Kim, C. Johnson, B. J. Vargo, P. K. Welch, M. Covington, P. K. A. Solomon, R. C. Newton, G. L. Trainor, C. P. Decicco, S. S. Ko, *J. Med. Chem.* **2002**, *45*, 3794–3804.
- [36] R. Krishnamurti, D. R. Bellew, G. K. S. Prakash, *J. Org. Chem.* **1991**, *56*, 984–989.
- [37] V. K. Aggarwal, A. Mereu, *J. Org. Chem.* **2000**, *65*, 7211–7212.
- [38] P. J. Atkins, V. Gold, W. N. Wassef, *J. Chem. Soc. Perkin Trans. 2* **1984**, 1247–1251.
- [39] O. Mitsunobu, *Synthesis*, **1981**, 1–28.
- [40] D. L. Hughes, *Org. React.* **1992**, *42*, 335–656.
- [41] E. Brunet, P. Garcia-Losada, J. C. Rodriguez-Ubis, O. Juanes, *Can. J. Chem.* **2002**, *80*, 169–174.
- [42] C. R. Cantor, P. R. Schimmel, *Biophysical Chemistry, Part II*, Freeman, New York, **1980**.
- [43] Y. R. Zhao, Q. Zheng, K. Dakin, K. Xu, M. L. Martinez, W.-H. Li, *J. Am. Chem. Soc.* **2004**, *126*, 4653–4663.
- [44] P. F. Wang, L. Jullien, B. Valeur, J.-S. Filhol, J. Canceill, J.-M. Lehn, *New J. Chem.* **1996**, *20*, 895–907.
- [45] D. Magde, E. L. Elson, W. W. Webb, *Phys. Rev. Lett.* **1972**, *29*, 705–708.
- [46] E. L. Elson, D. Magde, *Biopolymers* **1974**, *13*, 1–27.
- [47] D. Magde, E. L. Elson, W. W. Webb, *Biopolymers* **1974**, *13*, 29–61.
- [48] "Fluorescence Correlation Spectroscopy", N. L. Thompson, *Top. Fluoresc. Spectrosc.* **1991**, *1*, 337–410.
- [49] *Fluorescence Correlation Spectroscopy* (Eds.: R. Rigler, E. S. Elson), Springer Series in Chemical Physics, Springer, Berlin, **2001**.
- [50] E. L. Elson, *Traffic* **2001**, *2*, 789–796.
- [51] Y. Chen, J.-D. Müller, J.-S. Eid, E. Gratton in *New Trends in Fluorescence Spectroscopy, Applications to Chemical and Life Sciences* (Eds.: B. Valeur, J.-C. Brochon), Springer Series on Fluorescence, Methods and Applications, Springer, Berlin, **2001**, pp. 277–296.
- [52] N. L. Thompson, A. M. Lieto, N. W. Allen, *Curr. Opin. Struct. Biol.* **2002**, *12*, 634–641.
- [53] O. Krichinsky, G. Bonnet, *Rep. Prog. Phys.* **2002**, *65*, 251–297.
- [54] S. T. Hess, S. Huang, A. A. Heikal, W. W. Webb, *Biochemistry* **2002**, *41*, 697–705.
- [55] D. C. Lamb, A. Schenk, C. Röcker, C. Scalfi-Happ, G. U. Nienhaus, *Biophys. J.* **2000**, *79*, 1129–1138.
- [56] S. Charier, A. Meglio, D. Alcor, E. Cogné-Laage, J.-F. Allemand, L. Jullien, A. Lemarchand, *J. Am. Chem. Soc.* **2005**, *127*, 15491–15505.
- [57] B. Valeur, *Molecular Fluorescence Principles and Applications*, Wiley VCH, **2002**.
- [58] We did not consider the alternative Dexter mechanism for energy transfer in view of the absence of considerable coupling between the two considered chromophores.
- [59] S. Charier, O. Ruel, J.-B. Baudin, D. Alcor, J.-F. Allemand, A. Meglio, L. Jullien, *Angew. Chem.* **2004**, *116*, 4889–4892; *Angew. Chem. Int. Ed.* **2004**, *43*, 4785–4788.
- [60] S. Charier, O. Ruel, J.-B. Baudin, D. Alcor, J.-F. Allemand, A. Meglio, L. Jullien, B. Valeur, *Chem. Eur. J.* **2006**, *12*, 1097–1113.
- [61] E. W. P. Damen, T. J. Nevalainen, T. J. M. Van den Bergh, F. M. H. de Groot, H. W. Scheeren, *Bioorg. Med. Chem.* **2002**, *10*, 71–77.
- [62] J. N. Demas, G. A. Crosby, *J. Phys. Chem.* **1971**, *75*, 991–1024.
- [63] C. Gosse, A. Boutevine, I. Aujard, M. Chami, A. Kononov, E. Cogné-Laage, J.-F. Allemand, J. Li, L. Jullien, *J. Phys. Chem. B* **2004**, *108*, 6485–6497.
- [64] Lack of published results makes it difficult to discuss the values of the relative brightness of ncA^- with respect to nc , $\alpha(\lambda_{\text{exc}}^{(2)})$. The brightness after two-photon excitation is equal to the product of the quantum yield of fluorescence, $\Phi_{\text{F}}^{(2)}$, and the cross-section for two-photon absorption, δ . In the case of donor-acceptor fluorophores, one generally considers that the same emissive state is reached after one- and two-photon excitation, so that $\Phi_{\text{F}}^{(2)} = \Phi_{\text{F}}^{(1)}$ (ref.[31]). The data in Table 1 suggests $\Phi_{\text{F}}^{(1)}(\text{nc}) \approx \Phi_{\text{F}}^{(2)}(\text{nc}) \approx 0.1\%$ as an order of magnitude. It is more difficult to derive a range for the quantum

yield of fluorescence of the corresponding aci-nitro intermediates \mathbf{ncA}^- . In fact, the low quantum yield of fluorescence of the \mathbf{nc} caged species probably results from the presence of the nitro substituent. One could anticipate that the removal of the nitro substituent promotes an increase in the quantum yield of fluorescence of the corresponding aci-nitro intermediates \mathbf{ncA}^- . If one assumes that the latter lies within the same range as the esters of **12**, then $\Phi_F^{(1)}(\mathbf{ncA}^-) \approx \Phi_F^{(2)}(\mathbf{ncA}^-) \approx 10\%$. The derivation of the ratio $\delta(\lambda_{\text{exc}}^{(2)}, \mathbf{ncA}^-) / \delta(\lambda_{\text{exc}}^{(2)}, \mathbf{nc})$ is also difficult. Firstly, the relationship between molecular structure and $\delta(\lambda_{\text{max}}^{(2)})$ has not been established definitively; to derive a crude estimate, we assume $\delta(\lambda_{\text{max}}^{(2)}, \mathbf{ncA}^-) \approx \delta(\lambda_{\text{max}}^{(2)}, \mathbf{nc})$ in view of the similarity of the conjugated paths in \mathbf{ncA}^-

and \mathbf{nc} . We also take into account the expected red-shift that generally accompanies the conversion from the *ortho*-nitrobenzyl caged derivatives to the aci-nitro intermediates (ref. [25]). Upon considering that $\lambda_{\text{max}}^{(2)}$ is close to $2\lambda_{\text{max}}^{(1)}$ in donor-acceptor chromophores (refs. [31,32]) and that $\lambda_{\text{exc}}^{(2)}$ was generally larger than $2\lambda_{\text{max}}^{(1)}$ in the present work, we finally retained $\delta(\lambda_{\text{exc}}^{(2)}, \mathbf{ncA}^-) / \delta(\lambda_{\text{exc}}^{(2)}, \mathbf{nc}) \approx 1-10$. Thus, one obtains 10^2-10^3 as a crude estimate for $\alpha(\lambda_{\text{exc}}^{(2)})$. As shown in Table 2, the parameters calculated from the fit are in line with the preceding derivation.

Received: November 8, 2005

Revised: April 25, 2006

Published online: June 8, 2006